Bis-Hydrocarbyl Platinum(II) Ambiphilic Ligand Complexes: Alkyl–Aryl Exchange Between Platinum and Boron

*Bradley E. Cowie and David J. H. Emslie**

Department of Chemistry and Chemical Biology, McMaster University, 1280 Main Street West, Hamilton, Ontario, L8S 4M1, Canada.

ABSTRACT

Reaction of TXPB (2,7-di-*tert*-butyl-5-diphenylboryl-4-diphenylphosphino-9,9-dimethylthioxanthene) with [$PtMe_2$(COD)] (COD = 1,5-cyclooctadiene) yielded [PtMePh(TXPB')] (**1**; TXPB' = 2,7-di-*tert*-butyl-5-methylphenylboryl-4-diphenylphosphino-9,9-dimethylthioxanthene), presumably via undetected [$PtMe_2$(TXPB)]. The ambiphilic ligand in **1** is κ^2*PS*-coordinated, and the trigonal plane of the borane is oriented approximately parallel to the square plane at platinum. In solution, **1** is in equilibrium with zwitterionic [PtMe(TXPB-Me)] (**1'**) in which the *Pt*-phenyl group in **1** has been abstracted by the borane; the ratio of **1** to **1'** is approximately 90:10 at room temperature, and 50:50 at 183 K. The presence of **1'** in solution indicates that the pathway for phenyl–methyl exchange between platinum and boron involves a zwitterionic platinum(II) intermediate, rather than a platinum(IV) boryl complex resulting from B–C bond oxidative addition. Heating compound **1** provided an approximate 14:86 mixture of **1** and [$PtPh_2$(TXPB")] (**2**; TXPB" = 2,7-di-*tert*-butyl-5-dimethylboryl-4-diphenylphosphino-9,9-dimethylthioxanthene); **1** and **2** are in equilibrium at elevated temperature, and **2** is formed ($\Delta S^{\ddagger}$ = –45(12) J K^{-1} mol^{-1}; $\Delta H^{\ddagger}$ = 94(4) kJ mol^{-1}) *via* a second methyl–phenyl exchange between platinum and boron. The solid state structure of **2** is analogous to that of **1**, except with both phenyl groups on platinum and both methyl groups on boron. Compound **1** reacted with PPh_3 or $P(OPh)_3$ to afford neutral [PtMePh(L)(TXPB')] {L = PPh_3 (**3**) or $P(OPh)_3$ (**4**)} in which the TXPB' ligand is κ^1*P*-coordinated. However, **1** reacted with two equiv. of CNXyl (Xyl = 2,6-dimethylphenyl) to provide zwitterionic *trans*-[PtMe$(CNXyl)_2$(TXPB-Me)] (**5**; TXPB-Me is a κ^1*P*-coordinated anionic phosphine). This divergent reactivity is consistent with the accessibility of both neutral **1** and zwitterionic **1'** in solution.

Introduction

Bifunctional molecular complexes that contain either (a) a Lewis acidic metal center with one or more closely positioned Lewis basic site, or (b) a Lewis basic metal center with one or more closely positioned acidic proton or Lewis acidic lanthanide or transition metal center have been investigated extensively in homogeneous catalysis.[1] In contrast, molecular complexes containing a Lewis basic metal center with one or more appended main group Lewis acid have received far less attention, perhaps due to synthetic challenges associated with the synthesis of the ambiphilic ligands (ligands containing both Lewis basic and Lewis acidic groups) typically required to develop this area of research.

Early borane-containing ambiphilic ligands were generated in-situ by hydride transfer from a tris(*N*-methylthioimidazolyl)hydroborate monoanion to a coordinated metal.[2] This chemistry has been extended to include a broad range of hydroborate monoanions, and isolable borane-containing ambiphilic ligands have also been prepared. These ambiphilic ligands were used to access and characterize a diversity of metal–borane and metal–(co-ligand)–borane interactions,[3] and investigations into their potential in catalysis and small molecule activation have seen a recent surge in activity.[4-25] However, studies of the behavior of borane-containing ambiphilic ligands in combination with alkyl or aryl co-ligands[19-25] have received little attention (*vide infra*), despite the integral role of alkyl and aryl ligands in a large percentage of late transition metal catalysis.

In 2004, Tilley and Turculet described the reaction of [{PhB($CH_2P^iPr_2$)$_3$}Li(THF)] with 0.5 [{Rh(μ-Cl)(C_2H_4)$_2$}$_2$] to form [{κ^2-PhB($CH_2P^iPr_2$)$_2$}Rh(η^2-CH_2PPh_2)] (a in Figure 1). Addition of 2 equiv. of PMe_3 to this compound resulted in an equilibrium between the starting material and zwitterionic [{κ^2-PhB($CH_2P^iPr_2$)$_3$}Rh(PMe_3)$_2$] (b in Figure 1), providing an example of reversible alkyl transfer between rhodium and a pendant borane. Reaction of this equilibrium mixture with H_2 yielded zwitterionic *cis*-[{κ^3-PhB($CH_2P^iPr_2$)$_3$}RhH_2(PMe_3)] (c in Figure 1) whereas reaction with H_2SiPh_2 generated neutral [{κ^2-PhB($CH_2P^iPr_2$)$_2$}RhH_2($SiHPh_2$)(PMe_3)].[21]

In 2008, Tilley and Waterman reported the reaction of $Ph_2PCH_2CH_2BR_2$ (BR_2 = BCy_2 or BBN) with [(κ^2-dmpe)$PtMe_2$] to afford [(κ^2-dmpe)$PtMe(Ph_2PCH_2CH_2BR_2Me)$] (d in Figure 1); the product of alkyl abstraction by the borane. Zwitterionic [(κ^2-dmpe)$PtMe(Ph_2PCH_2CH_2BR_2Me)$] did not react with a 2nd equivalent of the ambiphilic ligand, and treatment with $B(C_6F_5)_3$ generated [(κ^2-dmpe)$PtMe(Ph_2PCH_2CH_2BR_2)$][$MeB(C_6F_5)_3$] with the remaining methyl group residing on the cationic platinum centre (e in Figure 1).[22] Erker also outlined the reactions of $Mes_2PCH_2CH_2B(C_6F_5)_2$ with [Cp_2ZrMe_2] and [$Cp^*_2ZrMe_2$], yielding zwitterionic [$Cp_2ZrMe\{\kappa^1$*P*-$Mes_2PCH_2CH_2B(C_6F_5)_2Me$)] in the former case and [Cp^*_2ZrMe][$MeB(C_6F_5)_2CH_2CH_2PMes_2$] (a contact ion pair in which the methyl group of the borate anion interacts with zirconium) in the latter.[23]

In 2008, Vedernikov reported that [{κ^2-$Me_2B(py)_2$}$PtMePh_2$] (f in Figure 1) is stable in benzene but isomerizes slowly in THF or DMSO to form [{κ^2-$MePhB(py)_2$}$PtMe_2Ph$] (g in Figure 1), in which the *B*-phenyl ring occupies the *endo* position with the *ipso* carbon η^1-bound to platinum. Similarly, [{κ^2-$Me_2B(py)_2$}$Pt(^{13}CH_3)Me_2$] (h in Figure 1) reacted slowly in DMSO to produce isomers in which the $^{13}CH_3$ group occupies either the *endo* or the *exo* position of the borate.[24] These reactivities achieve (a) alkyl/aryl exchange between boron and platinum(IV), with the aryl group migrating from platinum to boron, and (b) bidirectional alkyl exchange between boron and platinum(IV). Aryl group migration from boron to platinum was also observed in the reaction of Na[{κ^2-$Ph_2B(py)_2$}$PtMe_2$] with ^{i}PrOH (2 equiv.) and O_2 (0.5 equiv.) to form [{κ^3-$PhB(py)_2(O^iPr)$}$PtMe_2Ph$], NaO^iPr and H_2O. Analogous alkyl group migration was observed in the reactions of Na[{κ^2-$Me_2B(py)_2$}PtR_2] (R = Me or Ph) with EtOH and O_2, and [{κ^2-$Me_2B(py)_2$}PtR_2Me] (R = Me or Ph) was shown to react with MeOH to form [{κ^3-$MeB(py)_2(OMe)$}$PtRMe_2$] and HR.[24,25]

Herein we describe the synthesis and reactivity of bis-hydrocarbyl platinum(II) complexes bearing phosphine-thioether-borane ambiphilic ligands. These ligands are derived from 2,7-di-*tert*-butyl-5-diphenylboryl-4-diphenylphosphino-9,9-dimethylthioxanthene (TXPB)[13] through alkyl-aryl exchange between platinum and the borane in TXPB.

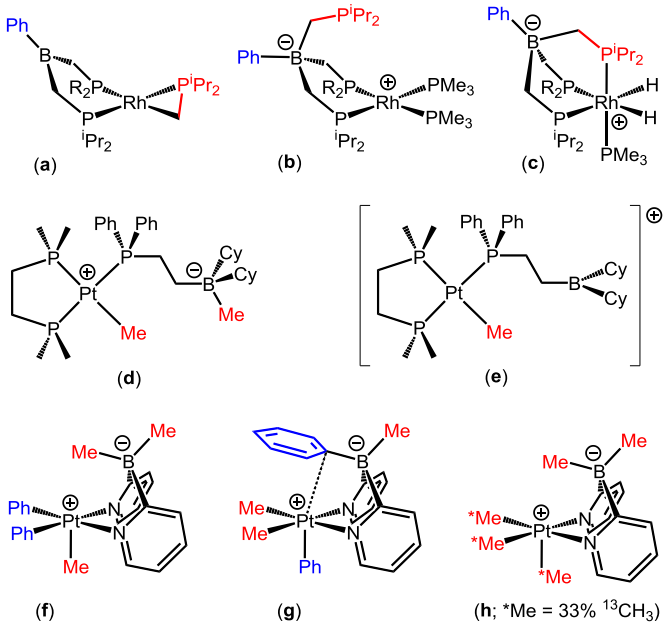

Figure 1. Late transition metal hydrocarbyl complexes bearing borane-containing ambiphilic ligands or anionic tetra(hydrocarbyl)borate ligands.[21,22,24]

Results and Discussion

[PtMePh(TXPB')]: Reaction of 2,7-di-*tert*-butyl-5-diphenylboryl-4-diphenylphosphino-9,9-dimethylthioxanthene (TXPB) with [$PtMe_2$(COD)] (COD = 1,5-cyclooctadiene) yielded [PtMePh(TXPB')] (**1**; TXPB' = 2,7-di-*tert*-butyl-5-methylphenylboryl-4-diphenylphosphino-9,9-dimethylthioxanthene) in which a methyl group on platinum has been exchanged for a phenyl group on boron (Scheme 1). The reaction proceeds over the course of 16 hours at room temperature, with no intermediates detectable by NMR spectroscopy. Single crystals of **1**·$(C_6H_{14})_{1.5}$ were grown from hexanes at –30 °C (Figure 2), highlighting a square planar geometry at platinum with the phenyl group *trans* to the phosphorus and the methyl group *trans* to sulphur. The Pt–P, Pt–S, Pt–C and B–C distances fall within the typical ranges,[26,27] and the trigonal plane of the borane is oriented approximately parallel to the square plane at platinum, with the *B*-phenyl group directed back towards platinum.

Scheme 1. Reaction scheme for the synthesis of [PtMePh(TXPB')] (**1**), [PtMe(TXPB-Me)] (**1'**) and [$PtPh_2$(TXPB")] (**2**).

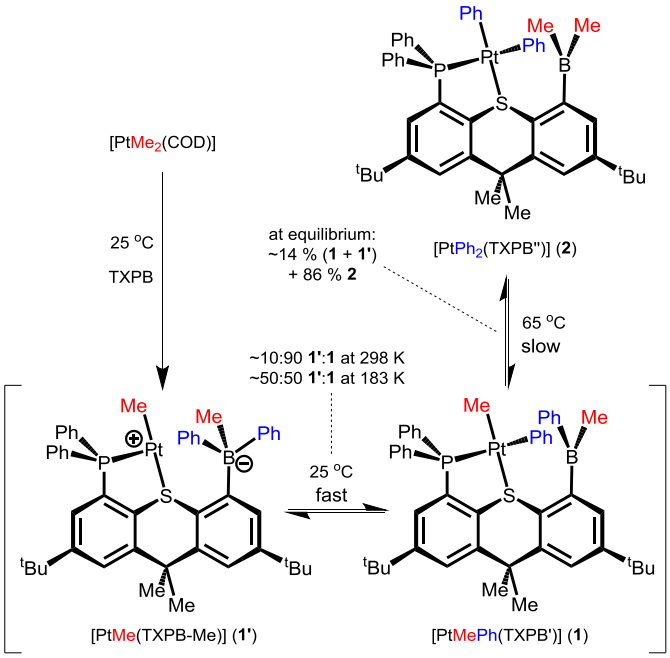

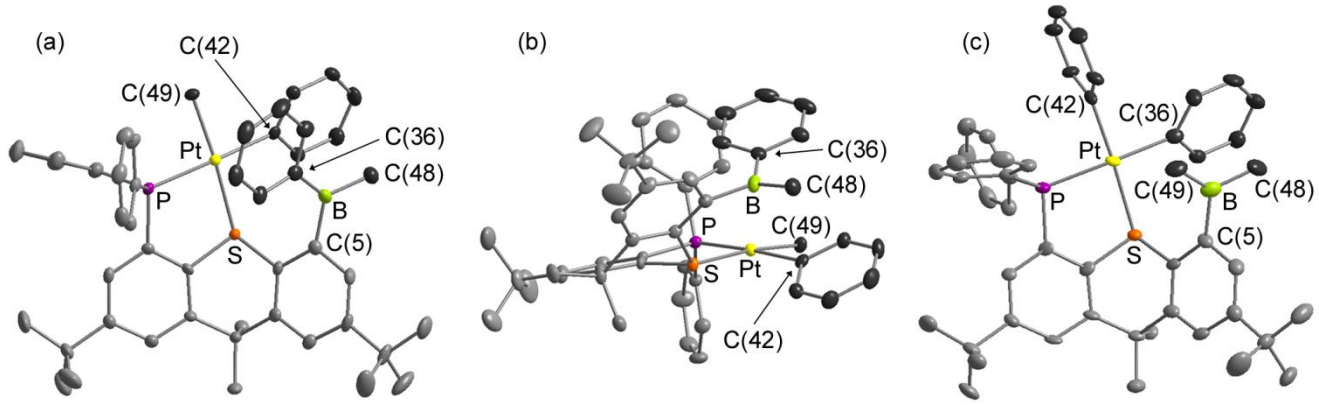

Figure 2. (a-b) X-ray crystal structure for **1**·$(C_6H_{14})_{1.5}$; bond distances (Å) and angles (°): Pt–P 2.272(1), Pt–S 2.320(1), Pt–C(42) 2.093(5), Pt–C(49) 2.066(5), Pt···B 3.655, B–C(5) 1.588(8), B–C(36) 1.561(8), B–C(48) 1.565(8), C(5)–B–C(36) 118.9(5), C(5)–B–C(48) 117.6(5), C(36)–B–C(48) 121.6(5), S–Pt–C(49) 172.7(1), P–Pt–C(42) 176.4(1), S–Pt–C(42) 94.2(1), S–Pt–P 86.09(4), P–Pt–C(49) 91.6(1), C(42)–Pt–C(49) 87.7(2). (c) X-ray crystal structure for **2**·$(CH_2Cl_2)(C_6H_{14})_{0.5}$; bond distances (Å) and angles (°): Pt–P 2.261(2), Pt–S 2.340(2), Pt–C(36) 2.065(9), Pt–C(42) 2.030(8), Pt···B 3.575, B–C(5) 1.59(1), B–C(48) 1.55(1), B–C(49) 1.55(1), C(5)–B–C(48) 117.4(8), C(5)–B–C(49) 117.7(8), C(48)–B–

C(49) 122.3(8), S–Pt–C(42) 176.9(2), P–Pt–C(36) 168.9(2), S–Pt–C(36) 93.2(2), S–Pt–P 86.08(7), P–Pt–C(42) 90.9(2), C(36)–Pt–C(42) 89.5(3). Hydrogen atoms, and solvent are omitted for clarity. Ellipsoids are set to 50 %.

Solid samples of **1** are pure by PXRD and elemental analysis. Additionally, room temperature ^{1}H, ^{13}C{^{1}H} and ^{31}P{^{1}H} NMR spectra of **1** in CD_2Cl_2 show single TXPB ligand and platinum environments, and two distinct methyl groups were observed in the ^{1}H NMR spectrum at 0.79 and 0.51 ppm; the former is sharp with platinum satellites ($^{2}J_{1H,195Pt}$ = 85 Hz) while the latter is a broad singlet, consistent with attachment to quadrupolar boron. However, the ^{31}P NMR signal (Figure 3), and the ^{13}C and ^{1}H NMR signals representing the Pt-phenyl and B-Phenyl groups are broadened at room temperature, suggesting an equilibrium between multiple species in solution.

Below –90 °C, two major isomers with vastly different $^{1}J_{195Pt,31P}$ coupling constants of 1958 and 5042 Hz were observed in an approximate 1:1 ratio, with ^{31}P chemical shifts of 38.7 and 36.4 ppm and ^{195}Pt chemical shifts of –4322 and –4700 ppm, respectively (Figure 3). The smaller $^{1}J_{195Pt,31P}$ coupling constant is consistent with neutral [PtMePh(TXPB')] (**1**; Scheme 1), where the phosphine is *trans* to a strongly donating hydrocarbyl ligand[28] (a similar ^{195}Pt NMR chemical shift and $^{1}J_{195Pt,31P}$ coupling was observed for neutral [$PtPh_2$(TXPB")] (**2**); *vide infra*). By contrast, the uncommonly large $^{1}J_{195Pt,31P}$ coupling constant is indicative of a phosphine *trans* to a very low *trans*-influence ligand or a vacant coordination site, accordant with zwitterionic [PtMe(TXPB-Me)] (**1'**; Scheme 1). For comparison, zwitterionic [(κ^2-dcpp)Pt{$CH_2CH_2B(C_6F_5)_3$}] {dcpp = 1,3-bis(dicyclohexylphosphino)propane}, which features a β-agostic C–H–Pt interaction, has $^{1}J_{195Pt,31P}$ couplings of 4755 and 2738 Hz, with the larger coupling constant assigned to the phosphine *trans* to the agostic interaction.[29] The $^{1}J_{195Pt,31P}$ coupling constant for **1'** is not consistent with a platinum(IV) tris-hydrocarbyl boryl complex (the product of B–C bond-breaking oxidative addition; **B** in Scheme 2; *vide infra*), since platinum(IV) complexes exhibit smaller $^{1}J_{195Pt,31P}$ coupling constants than closely related platinum(II) complexes.[30,31]

At 25 °C, the $^{13}C\{^{1}H\}$ NMR spectrum of **1-^{13}C** (**1** in which the methyl ligands are ^{13}C-labeled), revealed only two methyl-environments, representing B*Me* (13.1 ppm) and Pt*Me* (–1.9 ppm, $^{1}J_{13C,195Pt}$ = 767 Hz) groups. By contrast, at –90 °C, four methyl-environments were observed in the $^{13}C\{^{1}H\}$ NMR spectrum of **1-^{13}C**, only two of which exhibit platinum-satellites, consistent with isomers **1** and **1'** (Figure 3). The B*Me* signal for **1-^{13}C** is a broad singlet at 14.2 ppm ($\omega_{1/2}$ = 65 Hz), whereas the B*Me* signal for **1'-^{13}C** is a sharp singlet at 10.4 ppm, consistent with suppression of the quadrupolar broadening brought about by boron upon pyramidalization. In addition, while the Pt*Me* signal for **1-^{13}C** is observed at –5.5 ppm with a $^{1}J_{13C,195Pt}$ coupling of 585 Hz, the Pt*Me* signal for **1'-^{13}C** is located at –1.8 ppm with a $^{1}J_{13C,195Pt}$ coupling of 779 Hz, consistent with a stronger Pt–Me bond to the cationic platinum center in **1'**.

The ^{11}B NMR spectrum of **1** at –90 °C features a sharp singlet at –12 ppm, consistent with 4-coordinate boron (isomer **1'**), rather than a 3-coordinate borane or boryl ligand[32] (Figure 3; presumably the low temperature ^{11}B NMR signal for neutral **1** is too broad to be observed). By contrast, only a broad singlet at 63 ppm ($\omega_{1/2}$ = 3000 Hz) was observed in the ^{11}B NMR spectrum of **1** at 25 °C, suggesting that neutral **1** is the dominant isomer at room temperature. The magnitude of the $^{1}J_{31P,195Pt}$ coupling constant for solutions of **1** at 25 °C, relative to the $^{1}J_{31P,195Pt}$ coupling constants for isomers **1** and **1'** at –90 °C (*vide supra*), also suggests that **1** is the dominant isomer at room temperature, with an approximate 9:1 ratio of **1** to **1'**.

Taken together, the $^{195}Pt\{^{1}H\}$, $^{31}P\{^{1}H\}$, $^{13}C\{^{1}H\}$ and ^{11}B NMR data identify the two solution isomers as neutral **1** and zwitterionic **1'**. While isomer **1** was crystallographically characterized (*vide infra*), the structure and geometry of **1'** is unknown. However, it may bear resemblance to that of the previously reported [Rh(CO)(TXPB-F)] zwitterion (TXPB-F = {5-(2,7-di-*tert*-butyl-4-diphenylphosphino-9,9-dimethyl-thioxanthenyl)}diphenylfluoroborate), in which a *B*-phenyl ring is η^2*CC*-coordinated (via the *ipso* and one *ortho* carbon atom) to the cationic metal center.[33]

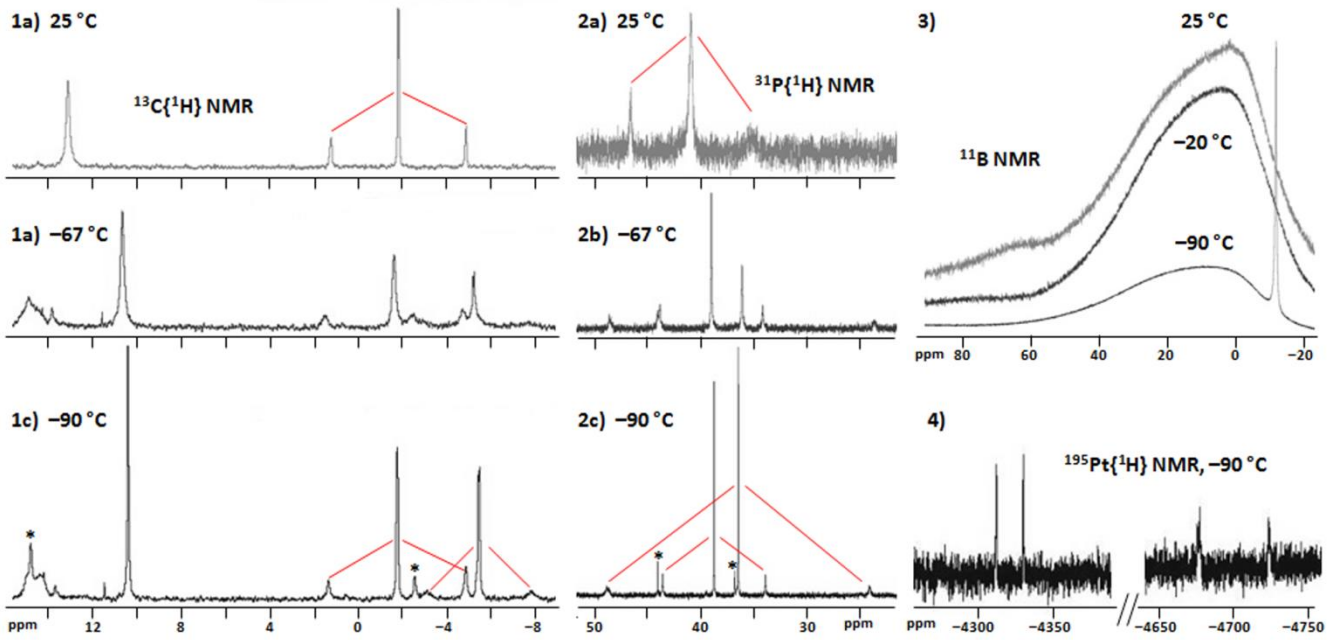

Figure 3. Variable temperature $^{13}C\{^{1}H\}$ NMR spectra of **1-^{13}C** (1a–1c), $^{31}P\{^{1}H\}$ NMR spectra of **1** (2a–2c), ^{11}B NMR spectra of **1** (3) and $^{195}Pt\{^{1}H\}$ NMR spectra of **1** (4) in CD_2Cl_2. Signals labeled with * represent an unidentified species.

In the reaction of TXPB with [$PtMe_2$(COD)], the initial product is presumably [$PtMe_2$(TXPB)] (**A**), which isomerizes rapidly to afford compound **1**. This reaction could proceed *via*: (a) a zwitterionic platinum(II) intermediate (**1'**) formed by abstraction of a methyl group from platinum by the pendant borane, or (b) a neutral platinum(IV) boryl intermediate (**B**) resulting from B–C bond oxidative addition (Scheme 2). The former pathway is indicated by the presence of an equilibrium between **1** and **1'** in solution, as evidenced by low temperature NMR spectroscopy (*vide supra*). The higher bond strength of Pt-aryl versus Pt-alkyl bonds likely provides the thermodynamic driving force for conversion of [$PtMe_2$(TXPB)] (**A**) to [PtMePh(TXPB')] (**1**). This reactivity contrasts that observed for [{κ^2-$Me_2B(py)_2$}$PtMePh_2$], in which phenyl/methyl exchange occurs to transfer a phenyl group from platinum to boron (*vide supra*); the driving force in this literature example is likely the formation of an η^1-arene interaction between platinum and the newly installed *B*-phenyl ring.

Scheme 2. Two possible reaction pathways to compound **1** proceeding (a) directly via intermediate **A**, or (b) via intermediates **A** and **B**. Only pathway 'a' is operative.

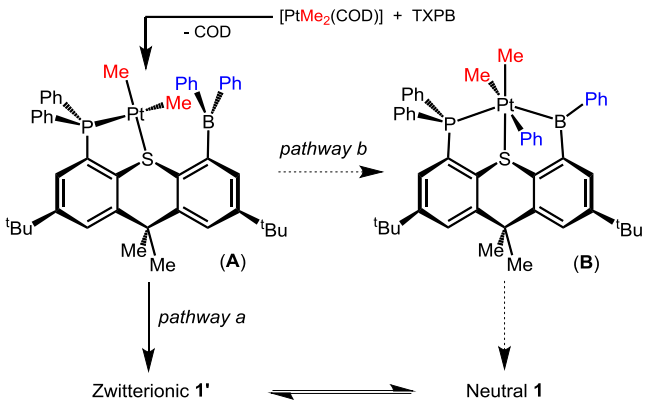

Thermal isomerization of 1: Heating a solution of compound **1** in CH_2Cl_2 at 65 °C or in C_6D_6 between 65 and 125 °C provided [$PtPh_2$(TXPB")] (**2**; TXPB" = 2,7-di-*tert*-butyl-5-dimethylboryl-4-diphenylphosphino-9,9-dimethylthioxanthene) as an approximate 86:14 mixture with remaining **1** (Scheme 1). Compound **1** could be completely removed from **2** by recrystallization from hexanes. However, **2** always contained 15 % of an unidentified neutral platinum(II) or platinum(IV) compound with a methyl group coordinated *cis* to the phosphine donor of TXPB.[34] X-ray quality crystals of **2**·$(CH_2Cl_2)(C_6H_{14})_{0.5}$ (Figure 2) were obtained from CH_2Cl_2/hexanes at –30 °C; the structure of **2** is very similar to that of **1**, but with two phenyl groups on platinum and two methyl substituents on boron. The ^{11}B and ^{195}Pt NMR chemical shifts for **2** are 80 and –4268 ppm, respectively, and the $^1J_{195Pt,31P}$ coupling is 1824 Hz. Unlike **1**, complex **2** does not participate in an NMR-detectable (25 to –80 °C) equilibrium with a zwitterionic isomer; this can be rationalized based on the requirement for aryl rather than alkyl anion abstraction from platinum in **2**, and the reduced Lewis acidity of the pendant borane in **2** (Ar–BMe_2), relative to the borane in **1** (Ar–BMePh).

Compound **2** is the result of a second methyl–phenyl exchange between platinum and boron (Schemes 1 and 3), and the ratio of **1** to **2** did not change by more than 2% over the temperature range investigated. Heating samples of **2** that did not contain **1** re-established the 86:14 ratio of compounds **2**

and **1**, respectively, confirming an equilibrium between **1** and **2** involving bidirectional transfer of alkyl and aryl groups between platinum and boron. Conversion of **1** to an equilibrium mixture of **1** and **2** was monitored in C_6D_6 by NMR spectroscopy between 65 and 125 °C in ten degree increments. At these elevated temperatures, [**1**] >> [**1'**] (*vide supra*), and reversible first order kinetic treatment $[([\mathbf{2}]_{eq}/[\mathbf{1}]_0)\ln\{[\mathbf{2}]_{eq}/([\mathbf{2}]_{eq}-[\mathbf{2}]_t)\} = kt]$[35] followed by Eyring analysis (Figure 4) provided values of 94(4) kJ mol^{-1} for $\Delta H^{\ddagger}$ and –45(12) J mol^{-1} K^{-1} for $\Delta S^{\ddagger}$ for the forward reaction.

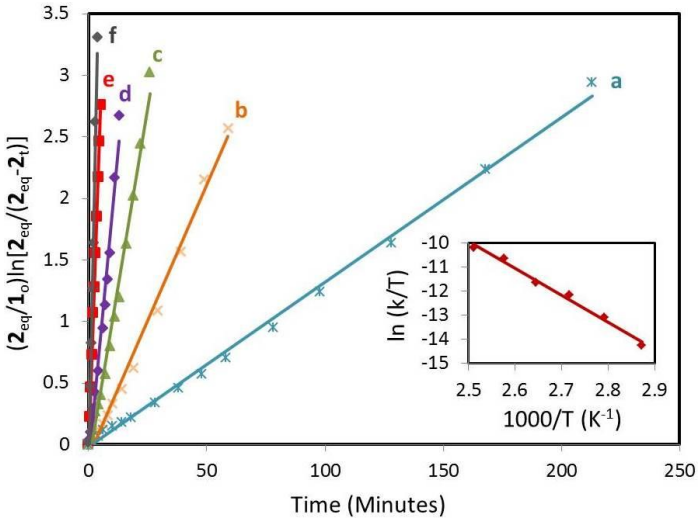

Figure 4. Reversible first order analyses for the thermal conversion of **1** to **2** in C_6D_6 at: (a) 75 °C (k = 2.12(2) × 10^{-4} s^{-1}), (b) 85 °C (k = 7.0(2) × 10^{-4} s^{-1}), (c) 95 °C (k = 1.83(5) × 10^{-3} s^{-1}), (d) 105 °C (k = 3.3(1) × 10^{-3} s^{-1}), (e) 115 °C (k = 8.93(9) × 10^{-3} s^{-1}), and (f) 125 °C (k = 1.49(9) × 10^{-2} s^{-1}). The inset shows an Eyring plot for the resulting rate data.

Possible reaction pathways from **1** to **2** are shown in Scheme 3. Pathway 'a' proceeds via a zwitterionic intermediate (**D** in Scheme 3) which is analogous to the zwitterionic intermediate (**1'**) between [$PtMe_2$(TXPB)] (**A**) and **1** (pathway 'a' in Scheme 2). However, prior to the formation of **D**, compound **1** must isomerize to form **C** in which the remaining Pt*Me* group is *trans* to phosphorus, and is therefore positioned in close proximity to the pendant borane (intermediate **C** in Scheme 3). If isomerization to form **C** does not take place, pathway 'b' involving B–C_{phenyl} bond cleaving oxidative

addition followed by B–C_{methyl} bond forming reductive elimination may be operative. The large negative $\Delta S^{\ddagger}$ is inconsistent with the formation of intermediate **C** in Scheme 3 via thioether dissociation. However, it is consistent with either (a) rate limiting isomerization to form **C** *via* a 5-coordinate intermediate, perhaps due to intramolecular coordination of platinum to the *B*-phenyl ring, or (b) concerted B–C_{phenyl} bond oxidative addition to form platinum(IV) intermediate **E** (pathway 'b' in Scheme 3).[36]

Scheme 3. Proposed reaction pathways for conversion of **1** to **2**: (a) via an isomer of **1** in which the platinum methyl group is trans to phosphorus (intermediate **C**), followed by abstraction of the platinum methyl group to form zwitterionic intermediate **D**, or (b) via platinum(IV) intermediate **E**.

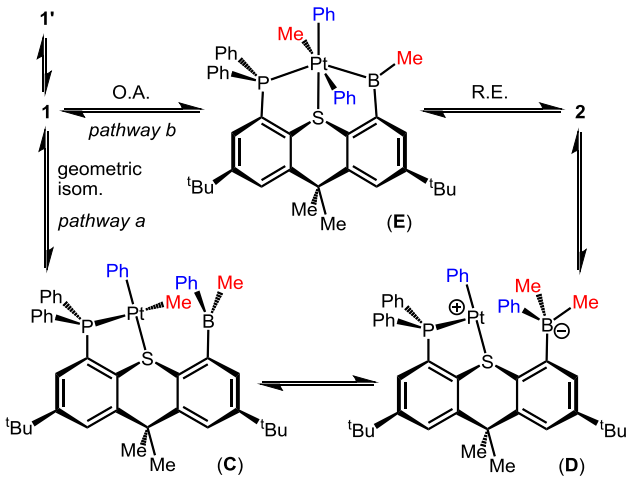

Reactions of 1 with Neutral Donors: Compound **1** reacted with one equiv. of PPh_3 or $P(OPh)_3$ to afford neutral [PtMePh(L)(TXPB')] {L = PPh_3 (**3**) or $P(OPh)_3$ (**4**)} in which the TXPB' ligand is κ^1P-coordinated and positioned *trans* to the phenyl group on platinum (Scheme 4). By contrast, **1** reacted with two equiv. of CNXyl (Xyl = 2,6-dimethylphenyl) to produce zwitterionic *trans*-[PtMe(CNXyl)$_2$(TXPB-Me)] (**5**; Scheme 4) in which TXPB-Me is a κ^1P-coordinated anionic phosphine and the isonitrile ligands are *trans* to one another (addition of 1 equiv. of CNXyl afforded a 1:1 mixture of **1** and **5**). These divergent reactivities are consistent with the accessibility of both neutral (**1**) and

zwitterionic (**1'**) species in solution.[37] Complexes **3** and **4** gave rise to ^{11}B NMR signals at 76 and ~82 ppm, respectively, consistent with a 3-coordinate borane. Conversely, the ^{11}B chemical shift for **5** is found at –10 ppm, indicative of an anionic borate. The ^{195}Pt chemical shifts for **3**–**5** are similar at –4569, –4495 and –4575, ppm, respectively.

Scheme 4. Reaction of **1**, which exists in equilibrium with **1'** in solution, with PPh_3, $P(OPh)_3$ and CNXyl. The reaction products are neutral **3** and **4**, and zwitterionic **5**.

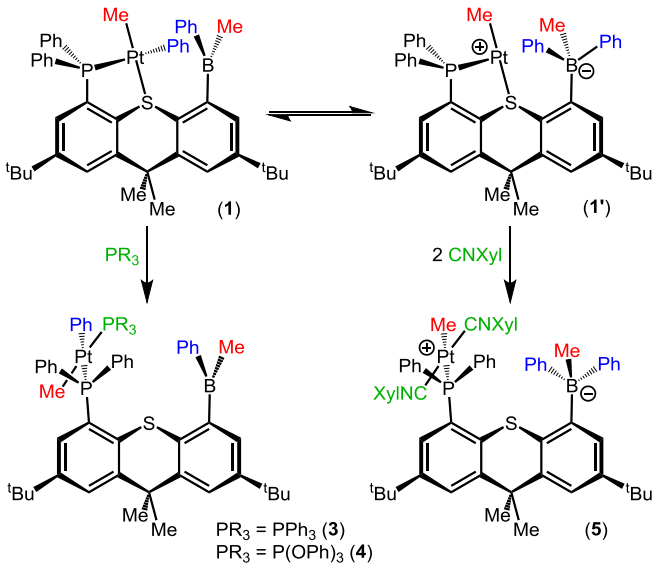

X-ray quality crystals of **4**·(1,2-$C_2H_4Cl_2$)$_{1.5}$ and **5**·(CH_2Cl_2)$_{2.6}$ were grown at –30 °C from 1,2-dichloroethane/hexanes and dichloromethane/hexanes, respectively (Figure 5).[38] Platinum is square planar in both complexes, but while boron is trigonal planar in **4**, it is tetrahedral in **5** with correspondingly elongated B–C bonds[39] (1.63-1.67 Å in **5** versus 1.57 Å in **4**). The neutral TXPB' and anionic TXPB-Me ligands in **4** and **5**, respectively, are κ^1*P*-coordinated to platinum, highlighting the lability of the central thioether donor. All Pt–C_{Ph}, Pt–C_{Me} and Pt–C_{CNR} distances in **4** and **5** are within expected ranges.[26,40] The Pt–PAr_3 and Pt–$P(OPh)_3$ distances in **4** are 2.2958(5) and 2.2204(5) Å, respectively, indicating stronger binding to the phosphite than the phosphine ligand. The Pt–PAr_3 bond in **5** [2.350(1) Å] is appreciably elongated relative to the Pt–PAr_3 bonds in **1**, **2** and **4** [2.261(2)-

2.2958(5) Å], consistent with less effective PAr_3 binding and more effective coordination of the *trans*-disposed methyl group, due to the positive charge at platinum.[41] Weaker phosphine coordination in **5** is also evidenced by an upfield shift of the ^{31}P NMR signal for the TXPB ligand (14.4 ppm vs 25-43 ppm in **1**-**4**) with a decreased $^{31}P–^{195}Pt$ coupling constant ($^{1}J_{31P,195Pt}$ = 1603 Hz vs 1698-1963 Hz in **1**-**4**).

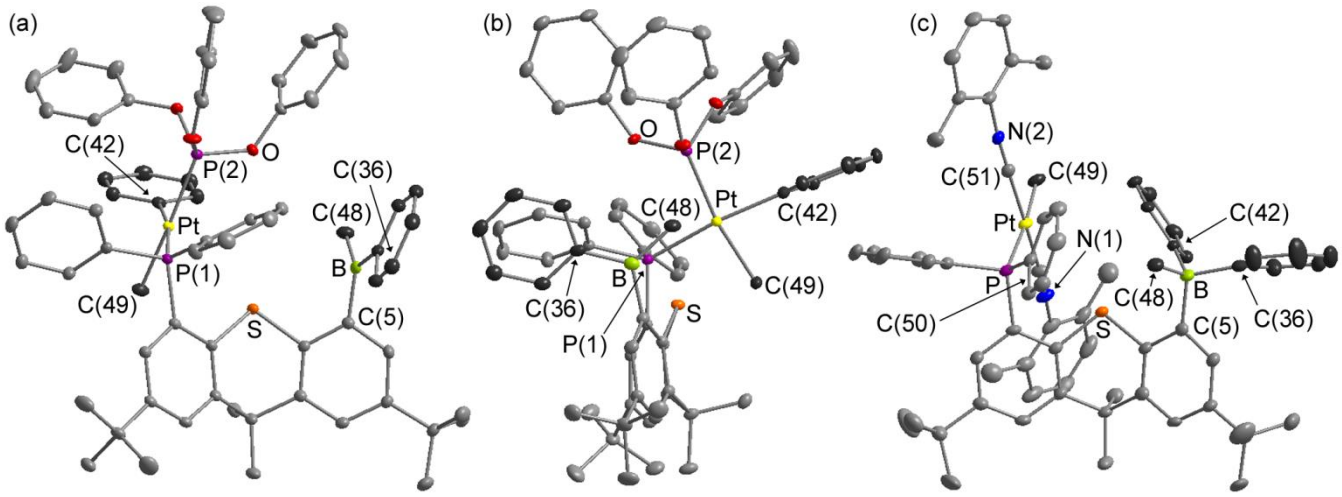

Figure 5. (a-b) X-ray crystal structure for **4**·$(1,2\text{-}C_2H_4Cl_2)_{1.5}$; bond distances (Å) and angles (°): Pt–P(1) 2.2958(5), Pt–P(2) 2.2204(5), Pt–C(42) 2.059(2), Pt–C(49) 2.101(2), Pt···B 5.471, B–C(5) 1.573(3), B–C(36) 1.566(3), B–C(48) 1.564(3), C(5)–B–C(36) 115.8(2), C(5)–B–C(48) 121.2(2), C(36)–B–C(48) 122.8(2), P(1)–Pt–C(42) 170.28(6), P(2)–Pt–C(49) 170.60(6), P(1)–Pt–P(2) 99.28(2), P(1)–Pt–C(49) 90.07(6), P(2)–Pt–C(42) 88.10(6), C(42)–Pt–C(49) 82.50(8). (c) X-ray crystal structure for **5**·$(CH_2Cl_2)_{2.6}$; bond distances (Å) and angles (°): Pt–P 2.3503(13), Pt–C(50) 1.940(4), Pt–C(51) 1.940(4), Pt–C(49) 2.117(5), Pt···B 5.850, C(50)–N(1) 1.156(6), C(51)–N(2) 1.151(6), B–C(5) 1.673(7), B–C(36) 1.648(7), B–C(42) 1.638(7), B–C(48) 1.631(7), C(5)–B–C(36) 108.4(4), C(5)–B–C(42) 109.3(4), C(5)–B–C(48) 108.0(4), C(36)–B–C(42) 109.4(4), C(36)–B–C(48) 110.0(4), C(42)–B–C(48) 111.7(4), P–Pt–C(49) 174.98(13), C(50)–Pt–C(51) 169.50(19), P–Pt–C(50) 96.19(15), P–Pt–C(51) 92.97(14), C(50)–Pt–C(49) 85.58(19), C(51)–Pt–C(49) 84.88(19). Hydrogen atoms and solvent are omitted for clarity. Ellipsoids are set to 50 %.

Summary and Conclusions

Reaction of TXPB with [$PtMe_2$(COD)] yielded [PtMePh(TXPB')] (**1**), which is converted to an approximate 14:86 mixture of **1** and [$PtPh_2$(TXPB")] (**2**) upon heating; **1** and **2** are in equilibrium at elevated temperatures. The *in-situ* generated TXPB' and TXPB" ambiphilic ligands are related to the original TXPB ligand through stepwise exchange of the phenyl groups on boron for methyl groups. In solution, compound **1** exists in equilibrium with a zwitterionic isomer, [PtMe(TXPB-Me)] (**1'**), and both solution species can be trapped by the addition of phosphines or isonitriles. Given the accessibility of both **1** and **1'** in solution, the reaction to form **1** from [$PtMe_2$(TXPB)] can be inferred to proceed via zwitterionic **1'**, rather than a platinum(IV) boryl intermediate. An analogous mechanism could potentially convert **1** to **2**, except that initial geometric isomerization would be required in order to position the remaining platinum methyl group in close proximity to the pendant borane. Application of reversible first order kinetics and Eyring analysis to the conversion of **1** to **2** gave a large negative $\Delta S^{\ddagger}$ of –45(12) J mol^{-1} K^{-1}, which is consistent with either (a) rate limiting formation of a 5-coordinate intermediate en route to isomer **C** in Scheme 3, followed by methyl group abstraction by the borane and subsequent transfer of the phenyl group on boron to platinum, or (b) concerted oxidative addition of a B–Ph bond, followed by B–Me bond forming reductive elimination. The reactivity described in this work provides examples of intramolecular alkyl abstraction by a pendant borane, reversible aryl abstraction by a pendant borane with spectroscopic identification and trapping of neutral and zwitterionic isomers, and *in-situ* generation of new ambiphilic ligands by stepwise alkyl/aryl exchange between platinum and boron. These alkyl/aryl exchange reactions differ fundamentally from those reported by Vedernikov *et al.* in that (a) they do not require strongly basic solvent to promote the exchange, and (b) the reactions en route to **1** and **1'** unambiguously maintain the platinum(II) oxidation state.

Experimental Section

General Details.

An argon-filled MBraun UNIlab glove box equipped with a −30 °C freezer was employed for the manipulation and storage of the TXPB ligand and its complexes, and reactions were performed on a double manifold high vacuum line using standard techniques.[42] A Fisher Scientific Ultrasonic FS-30 bath was used to sonicate reaction mixtures where indicated. Residual oxygen and moisture was removed from the argon stream by passage through an Oxisorb-W scrubber from Matheson Gas Products.

Anhydrous CH_2Cl_2 was purchased from Aldrich. Diethyl ether, pentane and hexanes were initially dried and distilled at atmospheric pressure from Na/Ph_2CO. Hexamethyldisiloxane {$O(TMS)_2$} was initially dried and distilled at atmospheric pressure from Na. Unless otherwise noted, all proteo solvents were stored over an appropriate drying agent (pentane, hexanes, $O(TMS)_2$ = Na/Ph_2CO/tetra-glyme; Et_2O = Na/Ph_2CO; CH_2Cl_2 = CaH_2) and introduced to reactions via vacuum transfer with condensation at −78 °C. Deuterated methylene chloride (ACP Chemicals) was dried over CaH_2.

The TXPB ligand,[13] $[PtCl_2(COD)]$,[43] $[PtMe_2(COD)]$ and $[Pt(^{13}C\text{-}Me)_2(COD)]$[44] were prepared according to literature procedures. 1,5-cyclooctadiene and $P(OPh)_3$ were purchased from Sigma-Aldrich and stored under argon following distillation from molecular sieves. $^{13}CH_3I$, Mg, MeMgI solution (3.0 M in Et_2O), CNXyl and PPh_3 were purchased from Sigma-Aldrich and either used as is or stored under argon. K_2PtCl_4 was purchased from Pressure Chemicals and used as is. Argon of 99.999 % purity was purchased from Praxair.

IR Spectra were recorded on a Thermo Scientific Nicolet 6700 FTIR spectrometer (reported stretches are strong unless otherwise noted). Combustion elemental analyses were performed on a Thermo EA1112 CHNS/O analyzer. A VWR Clinical 200 Large Capacity Centrifuge (with 28° fixed-angle rotors that hold 12 × 15 mL or 6 × 50 mL tubes) in combination with VWR high-performance polypropylene conical centrifuge tubes was used when required (inside the glovebox). NMR spectroscopy (^1H, $^{13}C\{^1H\}$, ^{11}B, $^{31}P\{^1H\}$, $^{195}Pt\{^1H\}$, DEPT-135, uDEFT, COSY, ^{13}C-EXSY, $^1H^{13}C$-HSQC, $^1H^{13}C$-HMBC) was performed on Bruker DRX-500 and AV-600 spectrometers. All ^1H NMR and ^{13}C NMR spectra were

referenced relative to $SiMe_4$ through a resonance of the employed deuterated solvent or proteo impurity of the solvent; 5.32 and 54.0 ppm for ^1H and ^{13}C NMR, respectively (CD_2Cl_2). ^{11}B, $^{31}P\{^1H\}$ and $^{195}Pt\{^1H\}$ NMR spectra were referenced using an external standard of $BF_3(OEt_2)$ (0.0 ppm), 85% H_3PO_4 in D_2O (0.0 ppm) and 1.2 M $Na_2[PtCl_6]$ in D_2O (0.0 ppm), respectively. Temperature calibration was performed using a d_4-methanol sample, as outlined in the Bruker VTU user manual.

Herein, numbered proton and carbon atoms refer to the positions of the thioxanthene backbone in the TXPB ligand. Inequivalent phenyl rings on boron and carbon are labeled A and B so that the proton and carbon resonances belonging to a single phenyl ring can be identified; we did not identify which *P*-phenyl ring gives rise to the signals labeled A or B. Platinum-195 satelites were not observed for the Pt*C*H_3 signals in the $^{13}C\{^1H\}$ NMR spectra of **3** and **4**, due to the low intensity of these peaks.

All rate constants for the conversion of **1** to **2** were determined by monitoring the ^1H NMR resonances of the TXPB-(C*Me*$_3$)$_2$ groups of complex **1** over the course of the reaction at a given temperature. In a typical experiment, complex **1** (7.6 mg, 8.3×10^{-3} mmol) and a small amount of ferrocene was dissolved in C_6D_6 (0.6 mL) in a sealed J-Young NMR tube. The NMR tube was fully submerged into an oil bath of the appropriate temperature (75, 85, 95, 105, 115 or 125 °C) and removed at the indicated time intervals for analysis of the reaction progression; to avoid extended periods of time at which NMR samples were still hot and the reaction could still proceed, albeit at reduced temperatures, NMR samples were immediately submerged under cold water once removed from the oil bath for data collection. The extent of reaction at each time interval was determined by integration of the peak intensity of the TXPB-(C*Me*$_3$)$_2$ resonances of complex **1** relative to ferrocene, which was present as an internal standard.

Due to the equilibrium between **1** and **2**, the rate constants for the conversion of **1** to **2** were determined by plotting $([\mathbf{2}]_{eq}/[\mathbf{1}]_o)[\ln([\mathbf{2}]_{eq}/[\mathbf{2}]_{eq}-[\mathbf{2}]_t)]$ versus time for a given temperature,[35] where $[\mathbf{2}]_{eq}$ is the equilibrium concentration of **2**, $[\mathbf{1}]_o$ is the initial concentration of **1**, and $[\mathbf{2}]_t$ is the concentration of **2** at time t (although $([\mathbf{2}]_{eq}/[\mathbf{1}]_o)[\ln([\mathbf{2}]_{eq}/[\mathbf{2}]_{eq}-[\mathbf{2}]_t)]$ vs time plots are shown with minutes as the units on the x-axis, rate constant values were obtained from plots with seconds as the x-axis units, or by dividing the slope of the lines on the former plots by 60). An Eyring plot was then constructured to determine the $\Delta H^{\ddagger}$

and $\Delta S^{\ddagger}$ values for the conversion of **1** to **2** (94(4) kJ mol^{-1} and –45(12) J mol^{-1} K^{-1}, respectively). Similarly, for the reverse reaction, $[([\mathbf{1}]_{eq}/[\mathbf{1}]_0)\ln\{[\mathbf{2}]_{eq}/([\mathbf{2}]_{eq}-[\mathbf{2}]_t)\} = k_{-1}t$, which gave a $\Delta H^{\ddagger}$ value of 97(4) kJ mol^{-1} and a $\Delta S^{\ddagger}$ value of –52(11) J mol^{-1} K^{-1}. The errors (σk) associated with the rates (k) for conversion of **1** to **2** were calculated in Excel using the 'linest' function: $k = 1.49(9)\times10^{-2}$ (125 °C), $8.93(9)\times10^{-3}$ (115 °C), $3.25(12)\times10^{-3}$ (105 °C), $1.83(5)\times10^{-3}$ (95 °C), $7.04(16)\times10^{-4}$ (85 °C) and $2.12(2)\times10^{-4}$ s^{-1} (75 °C). The errors in the activation parameters were computed from the following error propagation formulae: $(\sigma\Delta S)^2 = (R^2/\Delta T^2)\cdot\{(\sigma T/T)^2[T_{max}^2\{1 + T_{min}(\Delta L/\Delta T)\}^2 + T_{min}^2\{1 + T_{max}(\Delta L/\Delta T)\}^2] + (\sigma k/k)^2(T_{max}^2 + T_{min}^2)\}$ and $(\sigma\Delta H)^2 = \{(R^2T_{max}^2T_{min}^2)/(\Delta T^2)\}\cdot\{(\sigma T/T)^2[\{1 + T_{min}(\Delta L/\Delta T)\}^2 + \{1 + T_{max}(\Delta L/\Delta T)\}^2] + 2(\sigma k/k)^2\}$ where $\Delta T = (T_{max} - T_{min})$ and $\Delta L = [\{\ln(k_{max}/T_{max})\} - \{\ln(k_{min}/T_{min})\}]$.[45] A Fischerbrand thermometer (–20 to 150 °C, 305 mm length, 76 mm immersion) with an intrinsic accuracy of 1 °C was utilized, so the error associated with temperature (σT) was equal to 1.5 degrees.

X-ray crystallographic analyses were performed on suitable crystals coated in Paratone oil and mounted on a SMART APEX II diffractometer with a 3 kW Sealed tube Mo generator in the McMaster Analytical X-Ray (MAX) Diffraction Facility. In all cases, non-hydrogen atoms were refined anisotropically and hydrogen atoms were generated in ideal positions and then updated with each cycle of refinement. Anisotropic refinement of the molecule of 3-methylpentane and the half molecule of hexane in **1**·$(C_6H_{14})_{1.5}$, and the half molecule of hexane in **2**·$(CH_2Cl_2)(C_6H_{14})_{0.5}$ resulted in unstable refinement of the carbon atoms, therefore they were refined using the ISOR command. In addition, the carbon atoms of each respective solvent molecule were restrained to have similar thermal parameters through the use of the SIMU command. One molecule of CH_2Cl_2 {C(120), H(120), H(121), Cl(5), Cl(6)} in **5**·$(CH_2Cl_2)_{2.6}$ was refined with partial occupancy (60%). Powder X-ray diffraction (PXRD) experiments were performed on a Bruker D8 Advance powder diffractometer with Cu Kα radiation (λ = 0.154 nm) operated at 40 kV and 40 mA. Powders were packed in 0.5 mm o.d. special glass (SG; wall thickness 0.01 mm) capillary tubes for X-ray diffraction (purchased from Charles Supper Co.) and sealed by inverting to submerge the open end in a pool of Apiezon H-grease within a glovebox. The

calculated powder pattern for [PtMePh(TXPB')] was generated from the low-temperature single-crystal data and then refined using Topas 4.2 (Bruker software).

[PtMePh(TXPB')] (1): CH_2Cl_2 (20 mL) was condensed into a round bottom flask containing [$PtMe_2$(COD)] (173 mg, 0.518 mmol) and TXPB (356 mg, 0.518 mmol) through the use of a dry ice/acetone bath. The lemon yellow reaction solution was left to stir for 16 hours at room temperature (during which time the solution lost most of its colour, taking on only a slightly yellow tinge) before being evaporated to dryness *in vacuo*. Hexanes (15 mL) were condensed into the reaction flask and the oily suspension was sonicated for 15 minutes, after which point the hexanes solution was cooled to –78 °C for ~15 minutes then filtered while cold. The product was collected as a white solid and washed with hexanes (10 mL). Yield = 318 mg (67%). X-ray quality crystals of **1**·$(C_6H_{14})_{1.5}$ were obtained by cooling a solution of **1** in hexanes to –30 °C for several days. ^{1}H NMR (600 MHz, CD_2Cl_2, 298 K): δ 7.81 (s, 1H, C*H*^{1}), 7.67 (s, 1H, C*H*^{8}), 7.44–7.35 (m, 16H, C*H*^{3}, *o*,*m*,*p*-B*Ph*/Pt*Ph*, *o*,*m*,*p*-PPh_2), 6.90 (s, 1H, C*H*^{6}), 6.88 (broad s, 5H, *o*,*m*,*p*-B*Ph*/Pt*Ph*), 2.03 (s, 6H, CMe_2), 1.29, 1.26 (2 × s, 18H, 2 × CMe_3), 0.79 (d, $^2J_{H,Pt}$ 85, $^3J_{H,P}$ 6 Hz, 3H, Pt*Me*), 0.51 (broad s, 3H, B*Me*). ^{13}C{^{1}H} NMR (151 MHz, CD_2Cl_2, 298 K): δ 152.9 (d, $^3J_{C,P}$ 5 Hz, *C*^{2}), 150.0 (s, *C*^{7}), 146.7 (d, $^2J_{C,P}$ 11 Hz, *C*^{11}), 144.2 (s, *C*^{12}), 140.8 (d, $^1J_{C,P}$ 30 Hz, *C*^{4}), 136.8 (broad s, *o*,*m*,*p*-B*Ph*/Pt*Ph*), 133.7 (d, $^3J_{C,P}$ 10 Hz, *m*-PPh_2), 132.0 (d, $^1J_{C,P}$ 50 Hz, *ipso*-PPh_2), 130.7 (s, *p*-PPh_2), 130.5 (appt s, *C*^{10}), 129.5 (s, *C*^{3}), 129.0 (s, *C*^{13}), 128.7 (d, $^2J_{C,P}$ 10 Hz, *o*-PPh_2), 127.8 (broad s, *o*,*m*,*p*-BPh_2/Pt*Ph*), 126.4 (s, *C*^{6}), 125.8 (s, *C*^{1}), 122.1 (s, *C*^{8}), 43.5 (s, *C*Me_2), 35.3, 35.1 (2 × s, 2 × *C*Me_3), 31.5, 31.4 (2 × s, 2 × CMe_3), 26.0 (s, CMe_2), 12.9 (broad s, B*Me*), –2.0 (d, $^1J_{C,Pt}$ 767, $^2J_{C,P}$ 5 Hz, Pt*Me*); *ipso*-Pt*Ph*, *ipso*-B*Ph* and *C*^{5} could not be located. ^{31}P{^{1}H} NMR (203 MHz, CD_2Cl_2, 298 K): δ 40.9 (broad s, $^1J_{P,Pt}$ 2280 Hz). ^{31}P{^{1}H} NMR (203 MHz, CD_2Cl_2, 183 K): δ 38.7 (s, $^1J_{P,Pt}$ 1963 Hz). ^{11}B NMR (161 MHz, CD_2Cl_2, 298 K): δ 63 (broad s, $\omega_{1/2}$ 3000 Hz). ^{195}Pt{^{1}H} NMR (107 MHz, CD_2Cl_2, 183 K): δ –4322 (d, $^1J_{Pt,P}$ 1958 Hz). Anal. Calcd. For $C_{49}H_{54}BPPtS$ (%): C, 64.54; H, 5.97. Found: C, 64.37; H, 5.92.

Spectroscopic Data for [PtMe(TXPB-Me)] (1'): $^{31}P\{^{1}H\}$ NMR (203 MHz, CD_2Cl_2, 183 K): δ 36.4 (s, $^{1}J_{P,Pt}$ 5024 Hz). ^{11}B NMR (161 MHz, CD_2Cl_2, 183 K): δ –12 (s). $^{195}Pt\{^{1}H\}$ NMR (107 MHz, CD_2Cl_2, 183 K): δ –4700 (broad d, $^{1}J_{Pt,P}$ 5042 Hz, $\omega_{1/2}$ ~150 Hz).

[Pt(^{13}C-Me)Ph(TXPB'-^{13}C) (1-^{13}C): CH_2Cl_2 (10 mL) was condensed into a round bottom flask containing [Pt(^{13}C-Me)$_2$(COD)] (57.3 mg, 0.171 mmol) and TXPB (117 mg, 0.171 mmol) through the use of a dry ice/acetone bath. The lemon yellow reaction solution was left to stir for 16 hours at room temperature (during which time the solution lost most of its colour, taking on only a slightly yellow tinge) before being evaporated to dryness *in vacuo*. Hexanes (~10 mL) were condensed into the reaction flask and the oily suspension was sonicated for 15 minutes, after which point the hexanes solution was cooled to –78 °C for ~15 minutes then filtered while cold. The product was collected as a white solid and washed with hexanes (5 mL). Yield = 70.4 mg (45%). Key $^{13}C\{^{1}H\}$ NMR data for **1-^{13}C** (126 MHz, CD_2Cl_2, 298 K): δ 13.1 (s, B*Me*), –1.9 (d, $^{1}J_{C,Pt}$ 767 Hz, $^{2}J_{C,P}$ 5 Hz, Pt*Me*); $^{13}C\{^{1}H\}$ NMR (126 MHz, CD_2Cl_2, 183 K): δ 14.2 (broad s, $\omega_{1/2}$ 65 Hz, B*Me*), –5.5 (d, $^{1}J_{C,Pt}$ 586 Hz, $^{2}J_{C,P}$ 5 Hz, Pt*Me*). Key $^{13}C\{^{1}H\}$ NMR data for **1'-^{13}C** (126 MHz, CD_2Cl_2, 183 K): δ 10.4 (s, B*Me*), –1.8 (d, $^{1}J_{C,Pt}$ 779 Hz, $^{2}J_{C,P}$ 5 Hz, Pt*Me*). All other ^{1}H, $^{13}C\{^{1}H\}$ and $^{31}P\{^{1}H\}$ NMR data for **1-^{13}C** is consistent with that of **1** at 298 K and 183 K.

[PtPh$_2$(TXPB'')] (2): CH_2Cl_2 (10 mL) was condensed into a 50 mL Schlenk flask containing [PtMePh(TXPB')] (79.0 mg, 8.66×10^{-2} mmol) through the use of a dry ice/acetone bath. The reaction mixture was heated to 65 °C for 48 hours, after which the solvent was removed *in vacuo*. Hexanes (10 mL) were then condensed into the reaction flask and the oily residue was sonicated until fully dissolved; the hexanes solution was then brought into the dry box and stored at –30 °C for recrystallization. After 3 days a white powder had precipitated out of solution; the mother liquors were decanted and the resulting white solid was dried *in vacuo*. Crude yield = 48.9 mg {62%; this product did not contain **1**, but always contained ~15 % of an unidentified impurity which contains a Pt*Me* group *cis* to the phosphine donor of the TXPB ligand. The Pt-*Me* signal for the impurity is located at 0.32 ppm in the ^{1}H NMR spectrum in

CD_2Cl_2 ($^2J_{H,Pt}$ 72 Hz, $^3J_{H,P}$ 6 Hz), and the ^{t}Bu signals for this compound were singlets located at 1.29 and 1.24 ppm; the relative integration of these signals is 3H and 18H}. X-ray quality crystals of **2**·$(CH_2Cl_2)(C_6H_{14})_{0.5}$ were obtained by slow diffusion of hexanes into a solution of **2** in CH_2Cl_2 at –30 °C. ^{1}H NMR (500 MHz, CD_2Cl_2, 265 K): δ 7.74 (s, 1H, C*H*^{1}), 7.66 (d, $^3J_{H,H}$ 2 Hz, 1H, C*H*^{8}), 7.51 (t, $^3J_{H,Pt}$ 61 Hz, $^3J_{H,H}$ 6 Hz, 2H, *o*-Pt*Ph* A), 7.40–7.35 (m, 3H, C*H*^{3}, *p*-P*Ph*$_2$), 7.30–7.28 (m, 8H, *o*,*m*-P*Ph*$_2$), 7.09 (t, $^3J_{H,Pt}$ 74 Hz, $^3J_{H,H}$ 3 Hz, 2H, *o*-Pt*Ph* B), 6.92–6.86 (m, 3H, *m*,*p*-Pt*Ph* A), 6.82 (d, $^3J_{H,H}$ 2 Hz, 1H, C*H*^{6}), 6.79–6.77 (m, 3H, *m*,*p*-Pt*Ph* B), 2.02 (s, 6H, C*Me*$_2$), 1.27, 1.20 (2 × s, 18H, 2 × C*Me*$_3$), 0.61 (broad s, 6H, B*Me*$_2$). ^{13}C{^{1}H} NMR (126 MHz, CD_2Cl_2, 265 K): δ 155.5 (d, $^1J_{C,Pt}$ 112 Hz, *ipso*-Pt*Ph* A), 153.2 (d, $^3J_{C,P}$ 5 Hz, *C*^{2}), 151.4 (d, $^2J_{C,P}$ 9 Hz, *C*^{11}), 150.7 (s, *C*^{7}), 149.5 (s, *C*^{12}), 146.2 (d, $^3J_{C,P}$ 10 Hz, *C*^{10}), 145.1 (s, *C*^{13}), 140.7 (s, $^2J_{C,Pt}$ 33 Hz, *o*-Pt*Ph* A), 137.0 (s, $^2J_{C,Pt}$ 32 Hz, *o*-Pt*Ph* B), 133.8 (d, $^2J_{C,P}$ 12 Hz, *o*-P*Ph*$_2$), 131.4 (d, $^1J_{C,P}$ 49 Hz, *ipso*-P*Ph*$_2$), 130.7 (s, *p*-P*Ph*$_2$), 129.5 (s, *C*^{3}), 128.5 (d, $^3J_{C,P}$ 10 Hz, *m*-P*Ph*$_2$), 127.5 (appt. d, *J* 7 Hz, *m*-Pt*Ph* A), 127.5 (s, *m*-Pt*Ph* B), 126.0 (s, *C*^{1}), 124.1 (s, *p*-Pt*Ph* A), 123.9 (s, *C*^{6}), 123.0 (s, *C*^{8}), 122.0 (s, *p*-Pt*Ph* B), 43.6 (s, *C*Me$_2$), 35.1, 35.0 (2 × s, 2 × *C*Me$_3$), 31.4, 31.3 (2 × s, 2 × C*Me*$_3$), 25.8 (s, C*Me*$_2$), 16.6 (broad s, B*Me*$_2$); *ipso*-Pt*Ph* B, *C*^{4} and *C*^{5} could not be located. ^{31}P{^{1}H} NMR (203 MHz, CD_2Cl_2, 298 K): δ 42.7 (s, $^1J_{P,Pt}$ 1811 Hz). ^{11}B NMR (161 MHz, CD_2Cl_2, 298 K): δ 80 (broad s, $\omega_{1/2}$ ~2200 Hz). ^{195}Pt{^{1}H} NMR (128 MHz, CD_2Cl_2, 298 K): δ –4268 (d, $^1J_{Pt,P}$ 1824 Hz). Anal. Calcd. For $C_{49}H_{54}BPPtS$ (%): C, 64.54; H, 5.97. Found: C, 64.82; H, 6.36.

[PtMePh(PPh$_3$)(TXPB')] (3): CH_2Cl_2 (10 mL) was condensed into a round bottom flask containing [PtMePh(TXPB')] (92.6 mg, 0.102 mmol) through the use of a dry ice/acetone bath. A solution of PPh_3 (26.6 mg, 0.102 mmol) in CH_2Cl_2 (5 mL) was added dropwise at room temperature, and the resulting clear and colourless reaction solution was left to stir for 1 hour at room temperature before being evaporated to dryness *in vacuo* to yield an off-white oily residue. Hexanes (~20 mL) were added to the crude product, and the mixture was sonicated for 20 minutes before removal of the solvent *in vacuo*. Yield = 89.2 mg (75%). All attempts to acquire X-ray quality crystals of **3** resulted in preferential crystallization of *trans*-[$PtMe_2(PPh_3)_2$] (over the course of several days, the reaction of 2 equiv. of PPh_3

with **3** also formed a mixture of poorly soluble *trans*-[$PtMe_2(PPh_3)_2$], *trans*-[$PtMePh(PPh_3)_2$] (2:1 ratio) free TXPB, and free TXPB'). ^{1}H NMR (500 MHz, CD_2Cl_2, 298 K): δ 8.43 (d, $^3J_{H,P}$ 13 Hz, 1H, C*H*^{3}), 7.72 (s, 1H, C*H*^{1}), 7.56–7.50 (m, 4H, C*H*^{8}, *m*,*p*-B*Ph*), 7.33 (t, $^3J_{H,H}$ 7 Hz, 2H, *o*-B*Ph*), 7.18 (t, $^3J_{H,H}$ 9 Hz, 6H, *o*-P*Ph*$_3$), 7.10 (t, $^3J_{H,H}$ 7 Hz, 3H, *p*-P*Ph*$_3$), 7.03–6.92 (m, 15H, C*H*^{6}, *o*,*p*-P*Ph*$_2$, *o*-Pt*Ph*, *m*-P*Ph*$_3$), 6.79 (t, $^3J_{H,H}$ 6 Hz, 4H, *m*-P*Ph*$_2$), 6.50 (t, $^3J_{H,H}$ 7 Hz, 2H, *m*-Pt*Ph*), 6.41 (t, $^3J_{H,H}$ 7 Hz, 1H, *p*-Pt*Ph*), 1.71 (s, 6H, C*Me*$_2$), 1.37, 1.30 (2 × s, 18H, 2 × C*Me*$_3$), 1.11 (s, 3H, B*Me*), 0.22 (dd, $^2J_{H,Pt}$ 70 Hz, $^3J_{H,P}$ 9 Hz, $^3J_{H,P}$ 7 Hz, 3H, Pt*Me*). ^{13}C NMR (151 MHz, CD_2Cl_2, 298 K): δ 166.2 (dd, $^2J_{C,P}$ 114, 13 Hz, *ipso*-Pt*Ph*), 148.5 (s, *C*^{7}), 148.3 (d, $^3J_{C,P}$ 12 Hz, *C*^{2}), 144.8 (s, *C*^{5}), 143.3 (d, $^3J_{C,P}$ 5 Hz, *C*^{10}), 141.7 (s, *C*^{13}, *ipso*-B*Ph*), 137.5 (s, *m*-B*Ph*), 137.1 (s, $^2J_{C,Pt}$ 35 Hz, *o*-Pt*Ph*), 135.4 (broad s, *C*^{3}), 134.5 (d, $^2J_{C,P}$ 11 Hz, *o*-P*Ph*$_3$), 133.8 (broad s, *o*-P*Ph*$_2$), 133.0 (s, *p*-B*Ph*), 132.7 (s, *C*^{12}), 129.2 (s, *p*-P*Ph*$_3$), 129.0 (s, *p*-P*Ph*$_2$), 128.0 (s, *o*-B*Ph*), 127.6 (d, $^3J_{C,P}$ 9 Hz, *m*-P*Ph*$_2$, *m*-P*Ph*$_3$), 127.1 (s, *C*^{6}), 127.0 (d, $^4J_{C,P}$ 6 Hz, *m*-Pt*Ph*), 123.9 (s, *C*^{1}), 121.8 (s, *C*^{8}), 120.4 (s, *p*-Pt*Ph*), 41.2 (s, *C*Me$_2$), 35.3, 35.1 (2 × s, 2 × *C*Me$_3$), 31.6 (2 × s, 2 × C*Me*$_3$), 25.2 (s, C*Me*$_2$), 12.7 (s, B*Me*), 8.5 (dd, $^2J_{C,P}$ 94 Hz, $^2J_{C,P}$ 6 Hz, Pt*Me*); *ipso*-P*Ph*$_3$, *ipso*-P*Ph*$_2$, *C*^{4} and *C*^{11} could not be located. ^{31}P{^{1}H} NMR (203 MHz, CD_2Cl_2, 298 K): δ 24.6 (d, $^1J_{P,Pt}$ 1736 Hz, $^2J_{P,P}$ 11 Hz, Ar*P*Ph$_2$), 24.2 (d, $^1J_{P,Pt}$ 1916, $^2J_{P,P}$ 11 Hz, *P*Ph$_3$). ^{11}B NMR (161 MHz, CD_2Cl_2, 298 K): δ 76 (broad s, $\omega_{1/2}$ ~1900 Hz). ^{195}Pt{^{1}H} NMR (128 MHz, CD_2Cl_2, 298 K): δ –4569 (broad dd, $^1J_{Pt,P}$ 1957 Hz, $^1J_{Pt,P}$ 1767 Hz, $\omega_{1/2}$ ~120 Hz). Anal. Calcd. For $C_{67}H_{69}BP_2PtS$ (%): C, 68.53; H, 5.92. Found: C, 68.62; H, 6.39.

[PtMePh{P(OPh)$_3$}(TXPB')] (4): CH_2Cl_2 (10 mL) was condensed into a round bottom flask containing [PtMePh(TXPB')] (110 mg, 0.121 mmol) through the use of a dry ice/acetone bath. A solution of P(OPh)$_3$ (37.5 mg, 0.121 mmol) in CH_2Cl_2 (5 mL) was added dropwise at room temperature, and the resulting clear and colourless reaction solution was left to stir for 3 hours at room temperature before being evaporated to dryness *in vacuo* to yield an off-white oily residue. Hexamethyldisiloxane (~20 mL) was added to the crude product, and the mixture was sonicated for 20 minutes; the resulting slurry was brought into the dry box and stored at –30 °C to enable precipitation of the product. After several days a

white solid had precipitated out of solution; the mother liquors were decanted and the white powder was dried *in vacuo*. Yield = 86.2 mg (58%). X-ray quality crystals of **4**·1.5$C_2H_4Cl_2$ were obtained by slow diffusion of hexanes into a solution of **4** in $C_2H_4Cl_2$ at –30 °C (over the course of 3 days at room temperature, compound **4** reacted with 1.5 equiv. of $P(OPh)_3$ to form an approximate 2:1:1 mixture of **4**, *cis*-[$PtMe_2\{P(OPh)_3\}_2$] and free TXPB, as well as unreacted $P(OPh)_3$; this reaction was monitored by $^{31}P\{^1H\}$ NMR spectroscopy). ^1H NMR (600 MHz, CD_2Cl_2, 298 K): δ 7.69 (d, $^3J_{H,H}$ 7 Hz, 2H, *o*-B*Ph*), 7.60 (s, 1H, C*H*^{1}), 7.58–7.52 (m, 7H, C*H*^{3}, C*H*^{8}, *o*-P*Ph*$_2$, *p*-B*Ph*), 7.39 (t, $^3J_{H,H}$ 8 Hz, 2H, *m*-B*Ph*), 7.23 (dt, $^3J_{H,H}$ 8 Hz, $^4J_{H,H}$ 1 Hz, 2H, *p*-P*Ph*$_2$), 7.14 (dt, $^3J_{H,H}$ 8 Hz, $^4J_{H,P}$ 2 Hz, 4H, *m*-P*Ph*$_2$), 7.05–6.96 (m, 10H, C*H*^{6}, *m*,*p*-P(O*Ph*)$_3$), 6.91 (t, $^3J_{H,Pt}$ 61 Hz, $^3J_{H,H}$ 6 Hz, 2H, *o*-Pt*Ph*), 6.75–6.70 (m, 3H, *m*,*p*-Pt*Ph*), 6.50 (d, $^3J_{H,H}$ 8 Hz, 6H, *o*-P(O*Ph*)$_3$), 1.72 (s, 6H, C*Me*$_2$), 1.38 (s, 3H, B*Me*), 1.30, 1.14 (2 × s, 18H, 2 × C*Me*$_3$), 0.23 (t, $^2J_{H,Pt}$ 69 Hz, $^3J_{H,P}$ 10 Hz, 3H, Pt*Me*). ^{13}C NMR (151 MHz, CD_2Cl_2, 298 K): δ 158.9 (dd, $^2J_{C,P}$ 111 Hz, $^2J_{C,P}$ 15 Hz, *ipso*-Pt*Ph*), 152.1 (d, $^3J_{C,P}$ 11 Hz, *C*^{2}), 148.7 (s, *C*^{7}), 145.2 (s, *C*^{5}), 143.5 (d, $^3J_{C,P}$ 7 Hz, *C*^{10}), 141.8 (broad s, *ipso*-B*Ph*), 141.7 (s, *C*^{13}), 138.0 (s, *o*-Pt*Ph*), 137.8 (s, *o*-B*Ph*), 136.4 (d, $^2J_{C,P}$ 10 Hz, *C*^{11}), 135.5 (d, $^2J_{C,P}$ 11 Hz, *o*-P*Ph*$_2$), 133.3 (s, *p*-B*Ph*), 132.5 (s, *C*^{12}), 132.3 (d, $^1J_{C,P}$ 46 Hz, *ipso*-P*Ph*$_2$), 130.6 (d, $^2J_{C,P}$ 9 Hz, *C*^{3}), 130.1 (s, *p*-P*Ph*$_2$), 129.5 (s, *ipso*,*m*-P(O*Ph*)$_3$), 128.3 (s, *m*-B*Ph*), 128.2 (d, $^3J_{C,P}$ 10 Hz, *m*-P*Ph*$_2$), 127.3 (d, $^3J_{C,Pt}$ 66 Hz, $^4J_{C,P}$ 7 Hz, *m*-Pt*Ph*), 127.1 (s, *C*^{6}), 124.5 (s, *p*-P(O*Ph*)$_3$), 124.0 (s, *C*^{1}), 122.0 (s, *C*^{8}, *p*-Pt*Ph*), 121.1 (d, $^3J_{C,P}$ 5 Hz, *o*-P(O*Ph*)$_3$), 41.4 (s, *C*Me$_2$), 35.3, 35.2 (2 × s, 2 × *C*Me$_3$), 31.7, 31.5 (2 × s, 2 × C*Me*$_3$), 25.4 (s, C*Me*$_2$), 13.0 (s, B*Me*), 9.5 (dd, $^2J_{C,P}$ 149 Hz, $^2J_{C,P}$ 7 Hz, Pt*Me*); *C*^{4} could not be located. $^{31}P\{^1H\}$ NMR (203 MHz, CD_2Cl_2, 298 K): δ 108.1 (d, $^1J_{P,Pt}$ 3292 Hz, $^2J_{P,P}$ 18 Hz, *P*(OPh)$_3$), 25.4 (d, $^1J_{P,Pt}$ 1698 Hz, $^2J_{P,P}$ 18 Hz, Ar*P*Ph$_2$). ^{11}B NMR (161 MHz, CD_2Cl_2, 298 K): δ ~82 (broad s, $\omega_{1/2}$ ~ 4000 Hz). $^{195}Pt\{^1H\}$ NMR (128 MHz, CD_2Cl_2, 298 K): δ –4495 (dd, $^1J_{Pt,P}$ 3285 Hz, $^1J_{Pt,P}$ 1694 Hz). Anal. Calcd. For $C_{67}H_{69}BO_3P_2PtS$ (%): C, 65.84; H, 5.69. Found: C, 66.40; H, 6.48.

[PtMe(CNXyl)$_2$(TXPB-Me)] (5): CH_2Cl_2 (10 mL) was condensed into a round bottom flask containing [PtMePh(TXPB')] (83.8 mg, 9.19×10^{-2} mmol) through the use of a dry ice/acetone bath. A solution of

CNXyl (24.1 mg, 0.184 mmol) in CH_2Cl_2 (5 mL) was added dropwise at room temperature, and the resulting bright green/yellow reaction solution was left to stir for 5 hours at room temperature before being evaporated to dryness *in vacuo* to yield a bright green/yellow powder. Yield = 81.7 mg (76%). X-ray quality crystals of **5**·$(CH_2Cl_2)_{2.6}$ were obtained by slow diffusion of hexanes into a solution of **5** in CH_2Cl_2 at –30 °C. ^{1}H NMR (600 MHz, CD_2Cl_2, 298 K): δ 7.56–7.49 (m, 7H, C*H*^{1}, *o*,*p*-P*Ph*$_2$), 7.44 (dt, $^3J_{H,H}$ 8 Hz, $^4J_{H,P}$ 2 Hz, 4H, *m*-P*Ph*$_2$), 7.25 (d, $^3J_{H,H}$ 8 Hz, 4H, *o*-B*Ph*$_2$), 7.23 (s, 2H, *p*-Xyl), 7.07 (d, $^3J_{H,H}$ 8 Hz, 4H, *m*-Xyl), 7.00–6.97 (m, 6H, C*H*^{6}, C*H*^{8}, *m*-BPh$_2$), 6.83 (t, $^3J_{H,H}$ 7 Hz, 2H, *p*-B*Ph*$_2$), 6.70 (dd, $^3J_{H,P}$ 12 Hz, $^4J_{H,H}$ 2 Hz, 1H, C*H*^{3}), 2.06 (s, 12H, Xyl-*Me*), 1.24 (t, $^2J_{H,Pt}$ 48 Hz, $^3J_{H,P}$ 6 Hz, 3H, Pt*Me*), 1.22 (s, 6H, C*Me*$_2$), 1.08, 1.07 (2 × s, 18H, 2 × C*Me*$_3$), –0.13 (s, 3H, B*Me*). ^{13}C NMR (151 MHz, CD_2Cl_2, 298 K): δ 167.1 (broad s, *ipso*-B*Ph*$_2$), 147.3 (d, $^3J_{C,P}$ 8 Hz, *C*^{2}), 146.2 (s, *C*^{7}), 144.5 (d, $^3J_{C,P}$ 7 Hz, *C*^{10}), 140.8 (broad s, *C*NXyl), 139.8 (d, $^2J_{C,P}$ 14 Hz, *C*^{11}), 137.2 (s, *C*^{13}), 136.1 (s, *o*-Xyl), 135.6 (broad s, *C*^{5}), 134.8 (d, $^2J_{C,P}$ 12 Hz, *o*-P*Ph*$_2$), 134.4 (s, *o*-B*Ph*$_2$), 133.6 (s, *C*^{12}), 132.7 (s, *C*^{6}), 131.8 (s, *p*-P*Ph*$_2$), 130.7 (d, $^1J_{C,P}$ 50 Hz, *ipso*-P*Ph*$_2$), 130.6 (s, *p*-Xyl), 129.4 (d, $^3J_{C,P}$ 11 Hz, *m*-P*Ph*$_2$), 128.5 (s, *m*-Xyl), 128.1 (d, $^2J_{C,P}$ 5 Hz, *C*^{3}), 126.2 (s, *m*-B*Ph*$_2$), 124.6 (s, *C*^{1}), 122.3 (s, *ipso*-Xyl, *p*-B*Ph*$_2$), 115.8 (s, *C*^{8}), 40.5 (s, *C*Me$_2$), 35.0, 34.7 (2 × s, 2 × *C*Me$_3$), 31.7, 31.2 (2 × s, 2 × C*Me*$_3$), 25.4 (s, C*Me*$_2$), 18.7 (s, Xyl-*Me*), 11.3 (broad s, B*Me*), –9.6 (d, $^1J_{C,Pt}$ 393 Hz, $^2J_{C,P}$ 70 Hz, Pt*Me*); *C*^{4} could not be located. ^{31}P{^{1}H} NMR (203 MHz, CD_2Cl_2, 298 K): δ 14.4 (s, $^1J_{P,Pt}$ 1603 Hz). ^{11}B NMR (161 MHz, CD_2Cl_2, 298 K): δ –10 (s). ^{195}Pt{^{1}H} NMR (128 MHz, CD_2Cl_2, 298 K): δ –4575 (broad d, $^1J_{P,Pt}$ 1645 Hz, $\omega_{1/2}$ ~300 Hz). IR (C≡N), ν/cm^{-1}): 2170 (Nujol), 2181 (CH_2Cl_2). Anal. Calcd. For $C_{67}H_{72}BN_2PPtS$ (%): C, 68.53; H, 6.18; N, 2.39. Found: C, 68.31; H, 6.11; N, 2.88.

ASSOCIATED CONTENT

Supporting Information. X-ray structure refinement details for **1**, **2**, **4** and **5**, PXRD for **1**, multinuclear variable temperature NMR spectra for **1**-**5**, and rate plots for the conversion of **1** to **2**. CIF files for the X-ray structures are available free of charge *via* the internet at http://pubs.acs.org.

AUTHOR INFORMATION

Corresponding Author

* Phone: 905-525-9140, Fax: 905-522-2509. E-mail: emslied@mcmaster.ca.

ACKNOWLEDGMENT

D.J.H.E. thanks NSERC of Canada for a Discovery Grant and B.E.C. thanks the Government of Canada for an NSERC PGS-D scholarship. We are grateful to Natalie L. Huk for performing initial test reactions to form compound **1** and for obtaining a preliminary X-ray crystal structure of **1**, and to Jeffrey Price for PXRD.

REFERENCES

(1) (a) Shibasaki, M.; Kanai, M.; Matsunaga, S.; Kumagai, N. *Top. Organomet. Chem.* **2011**, *37*, 1. (b) Ikariya, T. *Top. Organomet. Chem.* **2011**, *37*, 31. (c) Gunanathan, C.; Milstein, D. *Top. Organomet. Chem.* **2011**, *37*, 55. (d) Warner, M. C.; Casey, C. P.; Bäckvall, J. E. *Top. Organomet. Chem.* **2011**, *37*, 85. (e) Zhao, B. G.; Han, Z. B.; Ding, K. L. *Angew. Chem. Int. Ed.* **2013**, *52*, 4744. (f) Schneider, S.; Meiners, J.; Askevold, B. *Eur. J. Inorg. Chem.* **2012**, 412. (g) van der Vlugt, J. I. *Eur. J. Inorg. Chem.* **2012**, 363. (h) Shibasaki, M.; Matsunaga, S. *Chem. Soc. Rev.* **2006**, *35*, 269.

(2) (a) Hill, A. F.; Owen, G. R.; White, A. J. P.; Williams, D. J. *Angew. Chem. Int. Ed.* **1999**, *38*, 2759. (b) Owen, G. R. *Chem. Soc. Rev.* **2012**, *41*, 3535.

(3) (a) Amgoune, A.; Bouhadir, G.; Bourissou, D. *Top. Curr. Chem.* **2013**, *334*, 281. (b) Amgoune, A.; Bourissou, D. *Chem. Commun.* **2011**, 859. (c) Bouhadir, G.; Amgoune, A.; Bourissou, D.

Adv. Organomet. Chem. **2010**, *58*, 1. (d) Kuzu, I.; Krummenacher, I.; Meyer, J.; Armbruster, F.; Breher, F. *Dalton Trans.* **2008**, 5836. (e) Fontaine, F.-G.; Boudreau, J.; Thibault, M. H. *Eur. J. Inorg. Chem.* **2008**, 5439. (f) Parkin, G. *Organometallics* **2006**, *25*, 4744. (g) Emslie, D. J. H.; Cowie, B. E.; Kolpin, K. B. *Dalton Trans.* **2012**, *41*, 1101.

(4) (a) MacMillan, S. N.; Harman, W. H.; Peters, J. C. *Chem. Sci.* **2014**, *5*, 590. (b) Harman, W. H.; Lin, T. P.; Peters, J. C. *Angew. Chem. Int. Ed.* **2014**, *53*, 1081. (c) Fong, H.; Moret, M. E.; Lee, Y.; Peters, J. C. *Organometallics* **2013**, *32*, 3053. (d) Anderson, J. S.; Rittle, J.; Peters, J. C. *Nature* **2013**, *501*, 84. (e) Anderson, J. S.; Moret, M. E.; Peters, J. C. *J. Am. Chem. Soc.* **2013**, *135*, 534. (f) Suess, D. L. M.; Tsay, C.; Peters, J. C. *J. Am. Chem. Soc.* **2012**, *134*, 14158. (g) Harman, W. H.; Peters, J. C. *J. Am. Chem. Soc.* **2012**, *134*, 5080. (h) Moret, M. E.; Peters, J. C. *Angew. Chem. Int. Ed.* **2011**, *50*, 2063. (i) Moret, M. E.; Peters, J. C. *J. Am. Chem. Soc.* **2011**, *133*, 18118.

(5) (a) Lu, Z. Y.; Williams, T. J. *Chem. Commun.* **2014**, *50*, 5391. (b) Lu, Z. Y.; Malinoski, B.; Flores, A. V.; Conley, B. L.; Guess, D.; Williams, T. J. *Catalysts* **2012**, *2*, 412. (c) Conley, B. L.; Williams, T. J. *Comments Inorganic Chem.* **2011**, *32*, 195. (d) Conley, B. L.; Williams, T. J. *J. Am. Chem. Soc.* **2010**, *132*, 1764.

(6) Tutusaus, O.; Ni, C. B.; Szymczak, N. K. *J. Am. Chem. Soc.* **2013**, *135*, 3403.

(7) Kameo, H.; Nakazawa, H. *Organometallics* **2012**, *31*, 7476.

(8) (a) Malacea, R.; Chahdoura, F.; Devillard, M.; Saffon, N.; Gomez, M.; Bourissou, D. *Adv. Synth. Catal.* **2013**, *355*, 2274. (b) Bebbington, M. W. P.; Bontemps, S.; Bouhadir, G.; Hanton, M. J.; Tooze, R. P.; van Rensburg, H.; Bourissou, D. *New J. Chem.* **2010**, *34*, 1556.

(9) (a) Boone, M. P.; Stephan, D. W. *Chem. Eur. J.* **2014**, *20*, 3333. (b) Boone, M. P.; Stephan, D. W. *J. Am. Chem. Soc.* **2013**, *135*, 8508.

(10) (a) Miller, A. J. M.; Labinger, J. A.; Bercaw, J. E. *Organometallics* **2011**, *30*, 4308. (b) Miller, A. J. M.; Labinger, J. A.; Bercaw, J. E. *Organometallics* **2010**, *29*, 4499. (c) Miller, A. J. M.; Labinger, J. A.; Bercaw, J. E. *J. Am. Chem. Soc.* **2008**, *130*, 11874. (d) Ostapowicz, T. G.; Merkens, C.; Holscher, M.; Klankermayer, J.; Leitner, W. *J. Am. Chem. Soc.* **2013**, *135*, 2104. (e) Jana, R.; Blacque, O.; Jiang, Y. F.; Berke, H. *Eur. J. Inorg. Chem.* **2013**, 3155. (f) Huang, S. H.; Wang, X. P.; Richmond, M. G. *J. Organomet. Chem.* **2012**, *700*, 103.

(11) Koren-Selfridge, L.; Londino, H. N.; Vellucci, J. K.; Simmons, B. J.; Casey, C. P.; Clark, T. B. *Organometallics* **2009**, *28*, 2085.

(12) Cowie, B. E.; Emslie, D. J. H. *Organometallics* **2013**, *32*, 7297.

(13) Emslie, D. J. H.; Blackwell, J. M.; Britten, J. F.; Harrington, L. E. *Organometallics* **2006**, *25*, 2412.

(14) (a) Lancaster, S. J.; Al-Benna, S.; Thornton-Pett, M.; Bochmann, M. *Organometallics* **2000**, *19*, 1599. (b) Crevier, T. J.; Bennett, B. K.; Soper, J. D.; Bowman, J. A.; Dehestani, A.; Hrovat, D. A.; Lovell, S.; Kaminsky, W.; Mayer, J. M. *J. Am. Chem. Soc.* **2001**, *123*, 1059.

(15) (a) Podiyanachari, S. K.; Kehr, G.; Muck-Lichtenfeld, C.; Daniliuc, C. G.; Erker, G. *J. Am. Chem. Soc.* **2013**, *135*, 17444. (b) Podiyanachari, S. K.; Frohlich, R.; Daniliuc, C. G.; Petersen, J. L.; Muck-Lichtenfeld, C.; Kehr, G.; Erker, G. *Angew. Chem. Int. Ed.* **2012**, *51*, 8830. (c) Rojas, R. S.; Peoples, B. C.; Cabrera, A. R.; Valderrama, M.; Frohich, R.; Kehr, G.; Erker, G.; Wiegand, T.; Eckert, H. *Organometallics* **2011**, *30*, 6372. (d) Herrmann, C.; Kehr, G.; Frohlich, R.; Erker, G. *Organometallics* **2008**, *27*, 2328. (e) Hill, M.; Erker, G.; Kehr, G.; Frohlich, R.; Kataeva, O. *J. Am. Chem. Soc.* **2004**, *126*, 11046. (f) Hill, M.; Kehr, G.; Frohlich, R.; Erker, G. *Eur. J. Inorg. Chem.* **2003**, 3583.

(16) (a) Dyson, G.; Zech, A.; Rawe, B. W.; Haddow, M. F.; Hamilton, A.; Owen, G. R. *Organometallics* **2011**, *30*, 5844. (b) Tsoureas, N.; Bevis, T.; Butts, C. P.; Hamilton, A.; Owen, G. R. *Organometallics* **2009**, *28*, 5222.

(17) (a) Crossley, I. R.; Hill, A. F.; Willis, A. C. *Organometallics* **2008**, *27*, 312. (b) Crossley, I. R.; Hill, A. F. *Dalton Trans.* **2008**, 201. (c) Crossley, I. R.; Hill, A. F.; Willis, A. C. *Organometallics* **2007**, *26*, 3891.

(18) (a) Pang, K.; Tanski, J. M.; Parkin, G. *Chem. Commun.* **2008**, 1008. (b) Pang, K.; Quan, S. M.; Parkin, G. *Chem. Commun.* **2006**, 5015. (c) Figueroa, J. S.; Melnick, J. G.; Parkin, G. *Inorg. Chem.* **2006**, *45*, 7056.

(19) The behaviour of $Me_2PCH_2AlMe_2$ ambiphilic ligands in nickel(II) and rhodium(III) methyl complexes has been described. (a) Fontaine, F.-G.; Zargarian, D. *J. Am. Chem. Soc.* **2004**, *126*, 8786. (b) Thibault, M. H.; Boudreau, J.; Mathiotte, S.; Drouin, F.; Sigouin, O.; Michaud, A.; Fontaine, F.-G. *Organometallics* **2007**, *26*, 3807. (c) Boudreau, J.; Fontaine, F.-G. *Organometallics* **2011**, *30*, 511.

(20) Phenylbis(oxazolinyl)borane [$PhB(Ox^{Me2})_2$] has been reported to react with $AlMe_3$ or ZnR_2 (R = Me, Ph or CH_2Ph) to provide a zwitterionic alkylphenylbis(oxazolinyl)borate complex via alkyl transfer to boron. By contrast, $PhB(Ox^{Me2})_2$ reacted with ZnR'_2 (R' = Et, ^{n}Pr or ^{i}Bu) to form a zwitterionic phenylbis(oxazolinyl)hydroborate complex by β-hydride abstraction. (a) Dunne, J.

F.; Manna, K.; Wiench, J. W.; Ellern, A.; Pruski, M.; Sadow, A. D. *Dalton Trans.* **2010**, *39*, 641. (b) Zhu, J.; Mukherjee, D.; Sadow, A. D. *Chem. Commun.* **2012**, *48*, 464.

(21) Turculet, L.; Feldman, J. D.; Tilley, T. D. *Organometallics* **2004**, *23*, 2488.

(22) Fischbach, A.; Bazinet, P. R.; Waterman, R.; Tilley, T. D. *Organometallics* **2008**, *27*, 1135.

(23) Fromel, S.; Kehr, G.; Frohlich, R.; Daniliuc, C. G.; Erker, G. *Dalton Trans.* **2013**, *42*, 14531.

(24) Khaskin, E.; Zavalij, P. Y.; Vedernikov, A. N. *J. Am. Chem. Soc.* **2008**, *130*, 10088.

(25) (a) Pal, S.; Vedernikov, A. N. *Dalton Trans.* **2012**, *41*, 8116. (b) Khaskin, E.; Zavalij, P. Y.; Vedernikov, A. N. *Angew. Chem. Int. Ed.* **2007**, *46*, 6309.

(26) (a) Colacot, T. J.; Teichman, R. A.; Cea-Olivares, R.; Alvarado-Rodriguez, J. G.; Toscano, R. A.; Boyko, W. J. *J. Organomet. Chem.* **1998**, *557*, 169. (b) Grice, K. A.; Kaminsky, W.; Goldberg, K. I. *Inorg. Chim. Acta* **2011**, *369*, 76. (c) Romeo, R.; Scolaro, L. M.; Plutino, M. R.; Romeo, A.; Nicolo, F.; Del Zotto, A. *Eur. J. Inorg. Chem.* **2002**, 629. (d) Dilworth, J. R.; von Beckh, C. A. M.; Pascu, S. I. *Dalton Trans.* **2005**, 2151. (e) Jamali, S.; Nabavizadeh, S. M.; Rashidi, M. *Inorg. Chem.* **2008**, *47*, 5441. (f) Rashidi, M.; Nabavizadeh, S. M.; Zare, A.; Jamali, S.; Puddephatt, R. J. *Inorg. Chem.* **2010**, *49*, 8435.

(27) (a) Muller, P.; Huck, S.; Koppel, H.; Pritzkow, H.; Siebert, W. *Z. Naturforsch. B* **1995**, *50*, 1476. (b) Hoefelmeyer, J. D.; Gabbai, F. P. *Organometallics* **2002**, *21*, 982.

(28) Pregosin, P. S., In *NMR in Organometallic Chemistry*, Wiley-VCH: Weinheim, 2012; Ch. 7.

(29) Bauer, J.; Braunschweig, H.; Dewhurst, R. D.; Radacki, K. *Chem. Eur. J.* **2013**, *19*, 8797.

(30) (a) Crumpton-Bregel, D. M.; Goldberg, K. I. *J. Am. Chem. Soc.* **2003**, *125*, 9442. (b) Bayler, A.; Canty, A. J.; Edwards, P. G.; Skelton, B. W.; White, A. H. *J. Chem. Soc. Dalton Trans.* **2000**, 3325.

(31) Still, B. M.; Anil Kumar, P. G.; Aldrich-Wright, J. R.; Price, W. S. *Chem. Soc. Rev.* **2007**, *36*, 665.

(32) Kays, D. L.; Aldridge, S. *Struct. Bond.* **2008**, *130: Contemporary Metal Boron Chemistry I*, 29.

(33) Cowie, B. E.; Emslie, D. J. H.; Jenkins, H. A.; Britten, J. F. *Inorg. Chem.* **2010**, *49*, 4060.

(34) Selected NMR spectroscopic data for the unidentified impurity in samples of **2**: ^{1}H NMR δ 0.32 ppm; $^{3}J_{1H,31P}$ = 6 Hz (c.f. 6 Hz for **1**), $^{2}J_{1H,195Pt}$ = 72 Hz (c.f. 85 Hz for **1**); ^{31}P NMR δ 46.9; $^{1}J_{31P,195Pt}$ = 1889 Hz (c.f. 1958 Hz for **1**). This impurity was not identified, and we were not able to determine whether or not it is an isomer in slow equilibrium with **2**.

(35) (a) Laidler, K. J. Chemical Kinetics, 3rd ed.; Harper & Row: New York, 1987. (b) Doherty, S.; Newman, C. R.; Rath; R. K.; van den Berg; J.-A.; Hardacre, C.; Nieuwenhuyzen, M.; Knight, J. G. *Organometallics* **2004**, *23*, 1055. (c) Leigh W. J.; Arnold, D. R. *Can. J. Chem.* **1981**, *59*, 609.

(36) (a) Jordan, R. B., Reaction Mechanisms of Inorganic and Organometallic Systems, 3 ed.; Oxford University Press: New York, 2007. (b) Crabtree, R. H., The Organometallic Chemistry of the Transition Metals, 3rd ed.; John Wiley & Sons: Toronto, 2001.

(37) By ^{1}H NMR spectroscopy, compound **1** did not react with ethylene (1 atm, 20 ^{o}C).

(38) All attempts to crystallize **3** yielded *trans*-[$PtMe_2(PPh_3)_2$] as clear and colourless needle-shaped crystals, with **3** and small amounts of *trans*-[$PtMePh(PPh_3)_2$], *trans*-[$PtMe_2(PPh_3)_2$] and free TXPB/TXPB' remaining in solution.

(39) Zhu, D. M.; Kochi, J. K. *Organometallics* **1999**, *18*, 161.

(40) (a) Vicente, J.; Arcas, A.; Fernandez-Hernandez, J. M.; Aullon, G.; Bautista, D. *Organometallics* **2007**, *26*, 6155. (b) Vicente, J.; Arcas, A.; Galvez-Lopez, M. D.; Jones, P. G. *Organometallics* **2006**, *25*, 4247.

(41) (a) Fujita, M.; Kim, W. H.; Sakanishi, Y.; Fujiwara, K.; Hirayama, S.; Okuyama, T.; Ohki, Y.; Tatsumi, K.; Yoshioka, Y. *J. Am. Chem. Soc.* **2004**, *126*, 7548. (b) Hinkle, R. J.; Stang, P. J.; Arif, A. M. *Organometallics* **1993**, *12*, 3510.

(42) Burger, B. J.; Bercaw J. E. *Vacuum Line Techniques for Handling Air-Sensitive Organometallic Compounds*. In *Experimental Organometallic Chemistry: A Practicum in Synthesis and Characterization*; Wayda, A. L., Darensbourg, M. Y., Eds.; ACS Symp. Ser.; American Chemical Society: Washington D.C., 1987, Vol. 357, pp 79-98.

(43) McDermott, J. X.; White, J. F.; Whitesides, G. M. *J. Am. Chem. Soc.* **1976**, *98*, 6521.

(44) Costa, E.; Pringle, P. G.; Ravetz, M. *Inorg. Synth.* **1997**, *31*, 284.

(45) Morse, P. M.; Spencer, M. D.; Wilson, S. R.; Girolami, G. S. *Organometallics* **1994**, *13*, 1646.

For Table of Contents Use Only

Bis-Hydrocarbyl Platinum(II) Ambiphilic Ligand Complexes: Alkyl–Aryl Exchange Between Platinum and Boron

Bradley E. Cowie and David J. H. Emslie*

TOC Graphic (up to 3.25 in. (8.5 cm) wide and 1.75 in. (4.75 cm) tall.**):**